Supplementary Material: In silico models accurately predict in vivo response for IL-6 blockade in head and neck cancer

Fereshteh Nazari[1] Alexandra Oklejas[2] Jacques E. Nör[2]
Alexander T. Pearson*[1] Trachette L. Jackson*[3]

Supplementary Material

EC-TC Model Equations

Our approach is based on our group's previously published framework [1, 2] that describes tumor angiogenesis, vascular tumor growth, and response to treatment focusing on the following levels: (1) Intracellular level: regulation of signaling pathways that are critical to cell proliferation, apoptosis, and migration; (2) Cellular level: cell-surface dynamics of receptor-ligand binding and receptor activation that lead to intracellular signal transduction cascades; and (3) Tissue level: dynamics of signaling chemicals and anti-cancer agents within the tissue, tumor growth dynamics, and tumor and vascular response to treatment. We use the strategy of isolation of key biological subsystems followed by integration of these components into our larger, modular framework. The VEGF, Bcl-2 and cellular crosstalk modules described below are the result of over a decade of modeling-experimental collaboration to isolate the parameters and calibrate the subsystems. The novel additions in this paper are the CSC, IL-6 and combination treatment optimization modules.

While the details of the VEGF, Bcl-2, and cellular crosstalk modules can be found in [2], we describe their key features below in relation to CSC driven tumor growth and therapy. We begin with a mathematical description of the interaction between endothelial and tumor cells by tracking the temporal changes in the cellular and molecular species listed in Table S2 below. Although these variables now form a fully integrated computational model they were carefully developed in a modular fashion following a systems biology-based approach. The modules are color coded as follows: VEGFR2 impact on ECs = red; CSC driven tumor growth = blue; VEGFR1-mediated

crosstalk = green; IL-6 impact on CSC = purple and Bcl-2 = cyan.

The modules describing VEGFR2 impact on ECs, Bcl-2 and VEGFR1-mediated crosstalk were calibrated and parameterized with data in [2] and the estimation techniques are discussed in detail in [3].

Human dermal microvascular endothelial cell (HDMEC) response to VEGF

It has been reported that VEGF and its natural receptors VEGFR1 and VEGFR2 are highly expressed in HNSCC and that VEGF-mediated signaling is a critical mediator of EC proliferation and migration [2, 4, 5, 6]. VEGF also induces enhanced Bcl-2 expression in tumor-associated ECs, which enhances their survival [refs]. Therefore, the rate of change of the HDMEC population (H) is chosen to be a function of the fractional occupancies of VEGFR2 per cell ($\phi_{H_{A_2}}$). Also the rate of endothelial cell death is assumed to be a decreasing function of intracellular Bcl-2 expression by ECs (B_H). Thus, we have:

$$\underbrace{\frac{dH}{dt}}_{\text{Endothelial cells}} = \underbrace{\alpha_H \phi_{H_{A2}}^{n_H} H}_{\substack{\text{Activated VEGFR2-mediated} \\ \text{proliferation}}} - \underbrace{\frac{\delta_H}{1+\beta_H B_H} H}_{\substack{\text{Bcl-2-mediated} \\ \text{apoptosis}}}, \tag{S1}$$

where, $\phi_{H_{A2}} = \frac{C_{H_{A2}}}{R^t_{H_{A2}} H}$, $C_{H_{A2}}$ is the amount of VEGF-VERFR2 complexes on the ECs, and $R^t_{H_{A2}}$ is the total number of VEGFR2 receptors per cell.

Vascular Fraction (V) and Oxygen Concentration ($N(t)$)

Following in part our work in [ref], oxygen concentration is assumed to be proportional to the vascular proportion of the tumor cell numbers defined as the percentage $V = 100H/(H+S+E+D)$. Here we take $N(t) = \sigma_F(t)V$ where

$$\sigma_F(t) = \sigma_N \frac{e^{(t-3)}}{1+e^{(t-3)}}$$

and σ_N denotes the proportionality constant relating the vessel fraction. In [ref] we assumed that EC presence immediately translated to oxygen availability. Here we relax that assumption by choosing the function σ_F, which gradually approaches to its maximum, σ_N. The rationale for choosing "3" in σ_F function is that it takes almost five or six days for human ECs to generate functional microvessel networks, connect to mouse vessels and begin blood flow. With "3" chosen, σ_F is approximately 0.95 at t=6 and is 1 with at least 8 digits of accuracy at t=13. It also takes three days for the function to reach half of its maximal. Thus, an increase in the proportion of ECs compared to the number of TCs results in an increase in the level of oxygenation within the tumor.

Cancer stem (S), progenitor (E) and terminally differentiated (D) cell response to Oxygen, IL-6 and Bcl-2

The CSC module, which describes the dynamics of stem, progenitor, and terminally differentiated cells, was first derived by our group in [1]. However, we are now modeling EC-TC scaffolds, which are initially hypoxic. Because we are now interested in the impact of human ECs and, subsequent functional blood vessels on tumor growth, we modify the cancer cell equations so that cellular proliferation and death are dependent on oxygen concentration, $N(t)$. This modification is based on our published crosstalk module [2], where the effects of oxygen pressure on tumor cell proliferation and survival are denoted by $\mathcal{H}(N-N_p)$ and $1+\mathcal{H}(N_d-N)$, respectively, where $\mathcal{H}(.)$ is a Heaviside function. That is, when the oxygen level is less than a critical threshold ($N < N_p$), tumor cells stop proliferating and a further decline in oxygen level (below N_d) results in a doubling of the death rate of the tumor cells. So, to be clear, we isolated CSC module in [1] and the crosstalk module in [2], now we integrate the two to create a more comprehensive model.

$$\underbrace{\frac{dS}{dt}}_{\text{Tumor stem cells}} = \underbrace{\alpha_S P_S(S,\phi_S) S\mathcal{H}(N-N_p)}_{\text{Stem cell self-renewal}} - \underbrace{\frac{\delta_S}{1+\gamma_S\phi_S} S[1+\mathcal{H}(N_d-N)]}_{\substack{\text{IL-6 \& Bcl-2 mediated} \\ \text{apoptosis}}}, \tag{S2}$$

where,

$$P_S(S,\phi_S) = \frac{(P_{S_{max}} - P_{S_{min}}(\phi_S))P_{N_s}^n}{P_{N_s}^n + S^n} + P_{S_{min}}(\phi_S),$$

$$P_{S_{min}}(\phi_S) = \mu_S \left(P_{S_{max}} - P^*_{S_{min}}\right)\phi_S + P^*_{S_{min}}$$

$$\underbrace{\frac{dE}{dt}}_{\substack{\text{Tumor}\\ \text{progenitor cells}}} = \underbrace{A_{in}\alpha_S\left[1 - P_S(S,\phi_S)\right]S\mathcal{H}(N-N_p)}_{\substack{\text{Amplified}\\ \text{stem cell differentiation}}} - \underbrace{\alpha_E E\mathcal{H}(N-N_p)}_{\substack{\text{Progenitor cell}\\ \text{differentiation}}} - \underbrace{\frac{\delta_E}{1+\gamma_E\phi_E}E[1+\mathcal{H}(N_d-N)]}_{\substack{\text{IL-6 \& Bcl-2 mediated}\\ \text{apoptosis}}} \tag{S3}$$

$$\underbrace{\frac{dD}{dt}}_{\substack{\text{Tumor}\\ \text{differentiated cells}}} = \underbrace{2\alpha_E E\ \mathcal{H}(N-N_p)}_{\substack{\text{progenitor cell}\\ \text{differentiation}}} - \underbrace{\frac{\delta_D}{1+\gamma_D\phi_D}D[1+\mathcal{H}(N_d-N)]}_{\substack{\text{IL-6 \& Bcl-2 mediated}\\ \text{apoptosis}}} \tag{S4}$$

IL-6 synthesis, binding and uptake

Once bound to its receptors, VEGF enhances expression level of Bcl-2 on endothelial cells [4, 5]. That Bcl-2 signaling induces IL-6 expression in endothelial cells [5]. Therefore, the last term in Eq. S5 describe the secretion of IL-6 by endothelial cells which is a function of fraction of activated VEGFR2 on endothelial cells. All the equations related to IL-6 binding dynamics are fully described in our previous work [1].

$$\begin{aligned}\underbrace{\frac{dL}{dt}}_{\text{IL-6}} = &- \underbrace{k_f L R_S}_{\substack{\text{IL-6 binding to}\\ \text{stem cells}}} + \underbrace{k_r C_S}_{\substack{\text{IL6 dissociation}\\ \text{from stem cells}}} - \underbrace{k_f L R_E}_{\substack{\text{IL-6 binding to}\\ \text{progenitor cells}}} + \underbrace{k_r C_E}_{\substack{\text{IL-6 dissociation}\\ \text{from progenitor cells}}}\\ &- \underbrace{k_f L R_D}_{\substack{\text{IL-6 binding to}\\ \text{differentiated cells}}} + \underbrace{k_r C_D}_{\substack{\text{IL-6 dissociation}\\ \text{from differentiated cells}}} - \underbrace{\lambda_L L}_{\text{IL-6 natural decay}}\\ &+ \underbrace{\rho_T(S+E+D)}_{\substack{\text{IL-6 Production}\\ \text{by tumor cells}}} + \underbrace{\rho_H \phi_{H_{A2}}^{n_L} H}_{\substack{\text{Bcl-2-mediated}\\ \text{IL-6 production}\\ \text{by ECs}}}\end{aligned} \tag{S5}$$

Eqs (S12), (S13) and (S14) model the temporal changes in free IL-6 receptors on each of the cell types that we are considering. The first two terms in each equation are the association and dissociation of IL-6 to IL-6R. The recycling terms describe the reactions by which IL-6 is used up in the processes of mediating its cellular response, and the free receptors are recycled back to the cell surface. Following the formulation in [], the last two terms in each equation describe the production of new free receptors as new cells are generated and the loss of these receptors as cells die. Definitions of $\mathscr{P}$ and $\mathscr{D}$ are given by:

$$\mathscr{P}_S(S,\phi_S) = \alpha_S P_S(S,\phi_S) S\mathcal{H}(N-N_p) \tag{S6}$$

$$\mathscr{P}_E(S,\phi_S) = A_{in}\alpha_S[1-P_S(S,\phi_S)] S\mathcal{H}(N-N_p) \tag{S7}$$

$$\mathscr{P}_D(E) = 2\alpha_E E\mathcal{H}(N-N_p), \tag{S8}$$

and,

$$\mathscr{D}_S(S,\phi_S) = \frac{\delta_S}{1+\gamma_S\phi_S} S[1+\mathcal{H}(N_d-N)] \tag{S9}$$

$$\mathscr{D}_E(E,\phi_E) = \frac{\delta_E}{1+\gamma_E\phi_E} E[1+\mathcal{H}(N_d-N)] + \alpha_E E\mathcal{H}(N-N_p) \tag{S10}$$

$$\mathscr{D}_D(D,\phi_D) = \frac{\delta_D}{1+\gamma_D\phi_D} D[1+\mathcal{H}(N_d-N)] \tag{S11}$$

Then we have:

$$\begin{aligned}\frac{dR_S}{dt} = &- \underbrace{k_f L R_S}_{\substack{\text{IL-6 binding to}\\ \text{stem cells}}} + \underbrace{k_r C_S}_{\substack{\text{IL-6 dissociation}\\ \text{from stem cells}}} + \underbrace{k_p C_S}_{\text{Recycling}} + \underbrace{R_{T_S}\mathscr{P}_S(S,\phi_S)}_{\substack{\text{Generation of new } R_S\\ \text{via cell proliferation}}} \\ &\underbrace{- \frac{R_S}{R_S+C_S} R_{T_S}\mathscr{D}_S(S,\phi_S)}_{\substack{\text{Loss of } R_S\\ \text{via cell death}}}\end{aligned} \tag{S12}$$

$$\frac{dR_E}{dt} = - \underbrace{k_f L R_E}_{\substack{\text{IL-6 binding to}\\ \text{progenitor cells}}} + \underbrace{k_r C_E}_{\substack{\text{IL-6 dissociation}\\ \text{from progenitor cells}}} + \underbrace{k_p C_E}_{\text{Recycling}} + \underbrace{R_{T_E}\mathscr{P}_E(S,\phi_S)}_{\substack{\text{Generation of new } R_E\\ \text{via cell proliferation}}}$$

$$- \underbrace{\frac{R_E}{R_E + C_E} R_{T_E} \mathscr{D}_E(E, \phi_E)}_{\substack{\text{Loss of } R_E \\ \text{via cell death}}} \tag{S13}$$

$$\frac{dR_D}{dt} = - \underbrace{k_f L R_D}_{\substack{\text{IL-6 binding to} \\ \text{differentiated cells}}} + \underbrace{k_r C_D}_{\substack{\text{IL-6 dissociation} \\ \text{from differentiated cells}}} + \underbrace{k_p C_D}_{\text{Recycling}} + \underbrace{R_{T_D} \mathscr{P}_D(E)}_{\substack{\text{Generation of new } R_D \\ \text{via cell proliferation}}}$$

$$- \underbrace{\frac{R_D}{R_D + C_D} R_{T_D} \mathscr{D}_D(D, \phi_D)}_{\substack{\text{Loss of } R_D \\ \text{via cell death}}} \tag{S14}$$

(S15)

Eqs (S16), (S17) and (S18) are analogous to the ones above, as they describe changes in receptor-ligand complexes on each cell type. Similarly, in these equations, the internalization terms describe the reactions by which the complex is internalized and the free receptors are recycled to the cell surface. The last term in each equation describes the loss of these receptor complexes due to cell death.

$$\frac{dC_S}{dt} = \underbrace{k_f L R_S}_{\text{IL-6 binding to } R_S} - \underbrace{k_r C_S}_{\substack{\text{IL-6 dissociation} \\ \text{from } R_S}} - \underbrace{k_p C_S}_{\text{Internalization}}$$

$$- \underbrace{\frac{C_S}{R_S + C_S} R_{T_S} \mathscr{D}_S(S, \phi_S)}_{\substack{\text{Loss of } C_S \\ \text{via cell death}}} \tag{S16}$$

$$\frac{dC_E}{dt} = \underbrace{k_f L R_E}_{\text{IL-6 binding to } R_E} - \underbrace{k_r C_E}_{\substack{\text{IL-6 dissociation} \\ \text{from } R_E}} - \underbrace{k_p C_E}_{\text{Internalization}}$$

$$- \underbrace{\frac{C_E}{R_E + C_E} R_{T_E} \mathscr{D}_E(E, \phi_E)}_{\substack{\text{Loss of } C_E \\ \text{via cell death}}} \tag{S17}$$

$$\frac{dC_D}{dt} = \underbrace{k_f L R_D}_{\text{IL-6 binding to } R_D} - \underbrace{k_r C_D}_{\substack{\text{IL-6 dissociation} \\ \text{from } R_D}} - \underbrace{k_p C_D}_{\text{Internalization}}$$

$$- \underbrace{\frac{C_D}{R_D + C_D} R_{T_D} \mathscr{D}_D(D, \phi_D)}_{\substack{\text{Loss of } C_D \\ \text{via cell death}}} \tag{S18}$$

Tumor and/or endothelial cell-secreted VEGF

Equation (S19) describes the association, at rate k^f_{H1} and k^f_{H2}, and dissociation, at rate k^r_{H1} and k^r_{H2} of VEGF (A) to its receptors (VEGFR1 and VEGFR2) on endothelial cells. VEGF is removed via natural decay at rate λ_A. The last two terms describes VEGF secretion by both endothelial and tumor cells, respectively. ECs have been shown to secrete VEGF under Bcl-2-mediated signaling (Kaneko et al. 2007); consequently, a Bcl-2-dependent production of VEGF by ECs is included. Further, tumor cells under hypoxic condition secret VEGF (Shweiki et al. 1995) and we, therefore, assume the hypoxia-mediated VEGF production by tumors in the last term. The production being "switched on" when the oxygen concentration (N) falls below a hypoxic threshold N_h and "switched off" if $N > N_h$. Combining these assumptions, the rate of change of VEGF may be expressed as follows:

$$\begin{aligned}\underbrace{\frac{dA}{dt}}_{\text{VEGF}} &= \underbrace{-k^f_{H1}R_{H_{A1}}A + k^r_{H1}C_{H_{A1}} - k^f_{H2}R_{H_{A2}}A + k^r_{H2}C_{H_{A2}}}_{\text{reaction with VEGFR1/2 on endothelial cells}} \\ &\quad - \underbrace{\lambda_A A}_{\substack{\text{natural}\\ \text{decay}}} + \underbrace{\alpha_A \frac{B_H}{1+\beta_A B_H}H}_{\substack{\text{Bcl-2-mediated production}\\ \text{by endothelial cells}}} + \underbrace{\frac{\nu_A}{1+e^{-\kappa_A(N_h-N)}}(S+E+D)}_{\substack{\text{hypoxia-mediated VEGF}\\ \text{production by stem/bulk cells}}} \end{aligned} \tag{S19}$$

VEGF uptake and binding by endothelial cells

The equations for VEGFR1 and VEGFR2 binding are given below and they are derived analogously to the equations given for IL-6R binding.

$$\begin{aligned}\underbrace{\frac{dR_{H_{A1}}}{dt}}_{\substack{\text{free-VEGFR1}\\ \text{receptors}\\ \text{on ECs}}} &= \underbrace{-k^f_{H1}R_{H_{A1}}A + k^r_{H1}C_{H_{A1}} + k^p_{H1}C_{H_{A1}}}_{\text{reaction with VEGF}} + \underbrace{R^t_{H_{A1}}\alpha_H \phi^{n_H}_{H_{A2}}H}_{\substack{\text{production due to}\\ \text{endothelial cell proliferation}}} \\ &\quad \underbrace{-\frac{R_{H_{A1}}}{R_{H_{A1}}+C_{H_{A1}}}R^t_{H_{A1}}\frac{\delta_H}{1+\beta_H B_H}H}_{\substack{\text{loss due to}\\ \text{endothelial cell apoptosis}}} \end{aligned} \tag{S20}$$

$$\underbrace{\frac{dR_{H_{A2}}}{dt}}_{\substack{\text{free-VEGFR2}\\ \text{receptors}\\ \text{on ECs}}} = \underbrace{-k^f_{H2}R_{H_{A2}}A + k^r_{H2}C_{H_{A2}} + k^p_{H2}C_{H_{A2}}}_{\text{reaction with VEGF}} + \underbrace{R^t_{H_{A2}}\alpha_H\phi^{n_H}_{H_{A2}}H}_{\substack{\text{production due to}\\ \text{endothelial cell proliferation}}}$$
$$\underbrace{-\frac{R_{H_{A2}}}{R_{H_{A2}}+C_{H_{A2}}}R^t_{H_{A2}}\frac{\delta_H}{1+\beta_H B_H}H}_{\substack{\text{loss due to}\\ \text{endothelial cell apoptosis}}}, \tag{S21}$$

$$\underbrace{\frac{dC_{H_{A1}}}{dt}}_{\substack{\text{VEGF-VEGFR1}\\ \text{complex}\\ \text{on ECs}}} = \underbrace{k^f_{H1}R_{H_{A1}}A - k^r_{H1}C_{H_{A1}} - k^p_{H1}C_{H_{A1}}}_{\substack{\text{VEGFR1 activation by VEGF}\\ \text{on endothelial cells}}} - \underbrace{\frac{C_{H_{A1}}}{R_{H_{A1}}+C_{H_{A1}}}R^t_{H_{A1}}\frac{\delta_H}{1+\beta_H B_H}H}_{\substack{\text{loss due to}\\ \text{endothelial cell apoptosis}}} \tag{S22}$$

$$\underbrace{\frac{dC_{H_{A2}}}{dt}}_{\substack{\text{VEGF-VEGFR2}\\ \text{complex}\\ \text{on ECs}}} = \underbrace{k^f_{H2}R_{H_{A2}}A - k^r_{H2}C_{H_{A2}} - k^p_{H2}C_{H_{A2}}}_{\substack{\text{VEGFR2 activation by VEGF}\\ \text{on endothelial cells}}} - \underbrace{\frac{C_{H_{A2}}}{R_{H_{A2}}+C_{H_{A2}}}R^t_{H_{A2}}\frac{\delta_H}{1+\beta_H B_H}H}_{\substack{\text{loss due to}\\ \text{endothelial cell apoptosis}}} \tag{S23}$$

The Bcl-family of proteins

Bcl-2 mRNA is constitutively expressed within ECs, and undergoes natural decay. VEGF signals through VEGFR1 and VEGFR2 on ECs and induces expression of Bcl-2 and the proangiogenic chemokines such as CXCL1 and CXCL8 in ECs. Combining these processes we obtain the following equations for Bcl-2 mRNA expression in ECs.

$$\underbrace{\frac{dB_H}{dt}}_{\substack{\text{Bcl-2 produced}\\ \text{by ECs}}} = \underbrace{\chi_H}_{\substack{\text{Constitutive}\\ \text{expression}\\ \text{by ECs}}} + \underbrace{\eta_H\frac{\phi^{n_B}_{H_{A2}}}{\omega^{n_B}_H+\phi^{n_B}_{H_{A2}}}}_{\substack{\text{Activated VEGFR2-}\\ \text{mediated production}\\ \text{by ECs}}} - \underbrace{\delta_B B_H}_{\substack{\text{natural}\\ \text{decay}}} \tag{S24}$$

Model Reduction

EC-TC cross-talk model can be reduced to the following model with five less equations by using the fact that,

$$R_S = R_{T_S}S - CS \tag{S25}$$

$$R_E = R_{T_E}E - CE \tag{S26}$$

$$R_D = R_{T_D}D - CD \tag{S27}$$

$$R_{H_{A1}} = R^t_{H_{A1}}H - C_{H_{A1}} \tag{S28}$$

$$R_{H_{A2}} = R^t_{H_{A2}}H - C_{H_{A2}} \tag{S29}$$

Thus, the reduced form of the model is given by:

$$\frac{dH}{dt} = \underbrace{\alpha_H \phi^{n_H}_{H_{A2}} H}_{\substack{\text{Activated VEGFR2-mediated} \\ \text{proliferation}}} - \underbrace{\frac{\delta_H}{1+\beta_H B_H} H}_{\substack{\text{Bcl-2-mediated} \\ \text{apoptosis}}} \tag{S30}$$

$$\frac{dS}{dt} = \underbrace{\alpha_S P_S(S,\phi_S) S\mathcal{H}(N-N_p)}_{\text{Stem cell self-renewal}} - \underbrace{\frac{\delta_S}{1+\gamma_S\phi_S} S[1+\mathcal{H}(N_d-N)]}_{\substack{\text{IL-6 \& Bcl-2 mediated} \\ \text{apoptosis}}} \tag{S31}$$

$$\frac{dE}{dt} = \underbrace{A_{in}\alpha_S\left[1-P_S(S,\phi_S)\right] S\mathcal{H}(N-N_p)}_{\substack{\text{Amplified} \\ \text{stem cell differentiation}}} - \underbrace{\alpha_E E\mathcal{H}(N-N_p)}_{\substack{\text{Progenitor cell} \\ \text{differentiation}}} - \underbrace{\frac{\delta_E}{1+\gamma_E\phi_E} E[1+\mathcal{H}(N_d-N)]}_{\substack{\text{IL-6 \& Bcl-2 mediated} \\ \text{apoptosis}}} \tag{S32}$$

$$\frac{dD}{dt} = \underbrace{2\alpha_E E\mathcal{H}(N-N_p)}_{\substack{\text{progenitor cell} \\ \text{differentiation}}} - \underbrace{\frac{\delta_D}{1+\gamma_D\phi_D} D[1+\mathcal{H}(N_d-N)]}_{\substack{\text{IL-6 \& Bcl-2 mediated} \\ \text{apoptosis}}} \tag{S33}$$

$$\underbrace{\frac{dL}{dt}}_{\text{IL-6}} = -\underbrace{k_f L R_S}_{\substack{\text{IL-6 binding to} \\ \text{stem cells}}} + \underbrace{k_r C_S}_{\substack{\text{IL6 dissociation} \\ \text{from stem cells}}} - \underbrace{k_f L R_E}_{\substack{\text{IL-6 binding to} \\ \text{progenitor cells}}} + \underbrace{k_r C_E}_{\substack{\text{IL-6 dissociation} \\ \text{from progenitor cells}}} - \underbrace{k_f L R_D}_{\substack{\text{IL-6 binding to} \\ \text{differentiated cells}}} + \underbrace{k_r C_D}_{\substack{\text{IL-6 dissociation} \\ \text{from differentiated cells}}} - \underbrace{\lambda_L L}_{\text{IL-6 natural decay}}$$

$$+\underbrace{\rho_T(S+E+D)}_{\substack{\text{IL-6 Production}\\ \text{by tumor cells}}} + \underbrace{\rho_H \phi_{H_{A2}}^{n_L} H}_{\substack{\text{Bcl-2-mediated}\\ \text{IL-6 production}\\ \text{by ECs}}} \tag{S34}$$

$$\frac{dC_S}{dt} = \underbrace{k_f L R_S}_{\text{IL-6 binding to } R_S} - \underbrace{k_r C_S}_{\substack{\text{IL-6 dissociation}\\ \text{from } R_S}} - \underbrace{k_p C_S}_{\text{Internalization}}$$

$$-\underbrace{C_S \mathscr{D}_S(\phi_S, B_S)}_{\substack{\text{Loss of } C_S\\ \text{via cell death}}} \tag{S35}$$

$$\frac{dC_E}{dt} = \underbrace{k_f L R_E}_{\text{IL-6 binding to } R_E} - \underbrace{k_r C_E}_{\substack{\text{IL-6 dissociation}\\ \text{from } R_E}} - \underbrace{k_p C_E}_{\text{Internalization}}$$

$$-\underbrace{C_E \mathscr{D}_E(\phi_E, B_E)}_{\substack{\text{Loss of } C_E\\ \text{via cell death}}} \tag{S36}$$

$$\frac{dC_D}{dt} = \underbrace{k_f L R_D}_{\text{IL-6 binding to } R_D} - \underbrace{k_r C_D}_{\substack{\text{IL-6 dissociation}\\ \text{from } R_D}} - \underbrace{k_p C_D}_{\text{Internalization}}$$

$$-\underbrace{C_D \mathscr{D}_D(\phi_D, B_D)}_{\substack{\text{Loss of } C_D\\ \text{via cell death}}} \tag{S37}$$

$$\frac{dA}{dt} = \underbrace{-k_{H1}^f R_{H_{A1}} A + k_{H1}^r C_{H_{A1}} - k_{H2}^f R_{H_{A2}} A + k_{H2}^r C_{H_{A2}}}_{\text{reaction with VEGFR1/2 on endothelial cells}}$$

$$-\underbrace{\lambda_A A}_{\substack{\text{natural}\\ \text{decay}}} + \underbrace{\alpha_A \frac{B_H}{1+\beta_A B_H} H}_{\substack{\text{Bcl-2-mediated production}\\ \text{by endothelial cells}}} + \underbrace{\frac{\nu_A}{1+e^{-\kappa_A(N_h-N)}}(S+E+D)}_{\substack{\text{hypoxia-mediated VEGF}\\ \text{production by stem/bulk cells}}} \tag{S38}$$

$$\frac{dC_{H_{A1}}}{dt} = \underbrace{k_{H1}^f R_{H_{A1}} A - k_{H1}^r C_{H_{A1}} - k_{H1}^p C_{H_{A1}}}_{\substack{\text{VEGFR1 activation by VEGF}\\ \text{on endothelial cells}}} - \underbrace{C_{H_{A1}} \frac{\delta_H}{1+\beta_H B_H}}_{\substack{\text{loss due to}\\ \text{endothelial cell apoptosis}}} \tag{S39}$$

$$\frac{dC_{H_{A2}}}{dt} = \underbrace{k_{H2}^f R_{H_{A2}} A - k_{H2}^r C_{H_{A2}} - k_{H2}^p C_{H_{A2}}}_{\substack{\text{VEGFR2 activation by VEGF}\\ \text{on endothelial cells}}} - \underbrace{C_{H_{A2}} \frac{\delta_H}{1+\beta_H B_H}}_{\substack{\text{loss due to}\\ \text{endothelial cell apoptosis}}} \tag{S40}$$

$$\frac{dB_H}{dt} = \underbrace{\chi_H}_{\substack{\text{Constitutive}\\ \text{expression}\\ \text{by ECs}}} + \underbrace{\eta_H \frac{\phi_{H_{A2}}^{n_B}}{\omega_H^{n_B} + \phi_{H_{A2}}^{n_B}}}_{\substack{\text{Activated VEGFR2-}\\ \text{mediated production}\\ \text{by ECs}}} - \underbrace{\delta_B B_H}_{\substack{\text{natural}\\ \text{decay}}} \tag{S41}$$

Developing Cisplatin-Therapy Model Equation

Cisplatin-induces death of tumor cells: in order to include the cisplatin-induced death of the tumor cells we use a standard Michaelis-Menten equation as a function of the concentration of cisplatin within tumor, X(t), and denoted by:

$$\begin{aligned} M_S(X) &= \delta_S(1-\epsilon)\left(\frac{1}{1+\gamma_S\phi_S}+\frac{\Pi_S X}{K_M^S+X}\right)S, \epsilon \neq 1 \\ M_E(X) &= \delta_E(1-\epsilon)\left(\frac{1}{1+\gamma_E\phi_E}+\frac{\Pi_E X}{K_M^E+X}\right)E, \epsilon \neq 1 \\ M_D(X) &= \delta_D(1-\epsilon)\left(\frac{1}{1+\gamma_D\phi_D}+\frac{\Pi_D X}{K_M^D+X}\right)D, \epsilon \neq 1 \end{aligned}$$

K_M^i, for $i =$ S, E and D, are representing the half maximal inhibitory of cisplatin concentration and Π_i, denotes the amount by which cisplatin can increase the maximum natural death rate of CSCs, PCs and DCs, respectively. The parameter ϵ determines the type of interaction between the two ligands (cisplatin and IL-6). If $\epsilon < 1$ then there are enhanced effects and if $\epsilon > 1$ then there are synergistic effects. For simplicity we assume $\epsilon = 0$.

Cisplatin enhances the self-renewal capacity of normal and cancer stem cells: as mentioned above, cisplatin can enhance the stemness of CSCs. In fact, cisplatin can increase the expression of Bmi-1, a member of the poly comb group family of transcriptional regulators that plays an essential role in stem cell fate decisions and regulates the self-renewal capacity of normal and CSCs [7]. Therefore, in order to integrate this feature of cisplatin, we add a positive feedback function of cisplatin concentration in tumor (X) to the self-renewal probability function of CSCs (P_S) as following:

$$\begin{aligned} P_S(S,\phi_S,X) &= \frac{(P_{S_{max}} - P_{S_{min}}(\phi_S,X))P_{N_s}^n}{P_{N_s}^n + S^n} + P_{S_{min}}(\phi_S), \\ P_{S_{min}}(\phi_S,X) &= \mu_S\left(P_{S_{max}} - P_{S_{min}}^*\right)\left(\phi_S + \frac{X}{K_S+X}\right) + P_{S_{min}}^* \end{aligned}$$

Thus, adding the above changes to the pre-treatment EC-TC model gives us the following set of ODEs named as cisplatin-therapy model:

$$\frac{dS}{dt} = \underbrace{\alpha_S P_S(S,\phi_S)S}_{\text{Stem cell self-renewal}} \underbrace{-\delta_S\left(\frac{1}{1+\gamma_S\phi_S}+\frac{\Pi_S X}{K_M^S+X}\right)S}_{\text{Stem cell death}}$$

$$\frac{dE}{dt} = \underbrace{A_{in}\alpha_S(1-P_S(S,\phi_S))S}_{\substack{\text{Amplified}\\ \text{stem cell differentiation}}} - \underbrace{\alpha_E E}_{\substack{\text{Progenitor cell}\\ \text{differentiation}}} \underbrace{-\delta_E\left(\frac{1}{1+\gamma_E\phi_E}+\frac{\Pi_E X}{K_M^E+X}\right)E}_{\text{progenitor cell death}}$$

$$\frac{dD}{dt} = \underbrace{2\alpha_E E}_{\substack{\text{progenitor cell}\\ \text{differentiation}}} \underbrace{-\delta_D\left(\frac{1}{1+\gamma_D\phi_D}+\frac{\Pi_D X}{K_M^D+X}\right)D}_{\text{differentiated cell death}}$$

$$\frac{dL}{dt} = -\underbrace{k_f L R_S}_{\substack{\text{IL6 binding to}\\ \text{stem cells}}} + \underbrace{k_r C_S}_{\substack{\text{IL6 dissociation}\\ \text{from stem cells}}} - \underbrace{k_f L R_E}_{\substack{\text{IL6 binding to}\\ \text{progenitor cells}}} + \underbrace{k_r C_E}_{\substack{\text{IL6 dissociation}\\ \text{from progenitor cells}}}$$
$$- \underbrace{k_f L R_D}_{\substack{\text{IL6 binding to}\\ \text{differentiated cells}}} + \underbrace{k_r C_D}_{\substack{\text{IL6 dissociation}\\ \text{from differentiated cells}}} - \underbrace{\lambda_L L}_{\text{IL6 natural decay}} + \underbrace{\rho_T(S+E+D)}_{\substack{\text{IL-6 Production}\\ \text{by tumor cells}}}$$

$$\frac{dR_S}{dt} = -\underbrace{k_f L R_S}_{\substack{\text{IL-6 binding to}\\ \text{stem cells}}} + \underbrace{k_r C_S}_{\substack{\text{IL-6 dissociation}\\ \text{from stem cells}}} + \underbrace{k_p C_S}_{\text{Recycling}} + \underbrace{R_{T_S}\mathscr{P}_{\mathscr{S}}(S,\phi_S)}_{\substack{\text{Generation of new } R_S\\ \text{via cell proliferation}}}$$
$$\underbrace{-\frac{R_S}{R_S+C_S}R_{T_S}\mathscr{D}_{\mathscr{S}}(S,\phi_S)}_{\substack{\text{Loss of } R_S\\ \text{via cell death}}}$$

$$\frac{dC_S}{dt} = +\underbrace{k_f L R_S}_{\text{IL6 binding to } R_S} - \underbrace{k_r C_S}_{\substack{\text{IL6 dissociation}\\ \text{from } R_S}} - \underbrace{k_p C_S}_{\text{Internalization}} \underbrace{-\frac{C_S}{R_S+C_S}R_{T_S}\mathscr{D}_{\mathscr{S}}(S,\phi_S)}_{\substack{\text{Loss of } C_S\\ \text{via cell death}}}$$

$$\frac{dR_E}{dt} = -\underbrace{k_f L R_E}_{\substack{\text{IL-6 binding to}\\ \text{progenitor cells}}} + \underbrace{k_r C_E}_{\substack{\text{IL-6 dissociation}\\ \text{from progenitor cells}}} + \underbrace{k_p C_E}_{\text{Recycling}} + \underbrace{R_{T_E}\mathscr{P}_{\mathscr{E}}(E,\phi_E)}_{\substack{\text{Generation of new } R_E\\ \text{via cell proliferation}}}$$
$$\underbrace{-\frac{R_E}{R_E+C_E}R_{T_E}\mathscr{D}_{\mathscr{E}}(E,\phi_E)}_{\substack{\text{Loss of } R_E\\ \text{via cell death}}}$$

$$\frac{dC_E}{dt} = +\underbrace{k_f L R_E}_{\text{IL6 binding to } R_E} - \underbrace{k_r C_E}_{\substack{\text{IL6 dissociation}\\ \text{from } R_E}} - \underbrace{k_p C_E}_{\text{Internalization}} \underbrace{-\frac{C_E}{R_E+C_E}R_{T_E}\mathscr{D}_{\mathscr{E}}(E,\phi_E)}_{\substack{\text{Loss of } C_E\\ \text{via cell death}}}$$

$$\frac{dR_D}{dt} = -\underbrace{k_f L R_D}_{\substack{\text{IL-6 binding to}\\ \text{differentiated cells}}} + \underbrace{k_r C_D}_{\substack{\text{IL-6 dissociation}\\ \text{from differentiated cells}}} + \underbrace{k_p C_D}_{\text{Recycling}} + \underbrace{R_{T_D}\mathscr{P}_{\mathscr{D}}(E,\phi_D)}_{\substack{\text{Generation of new } R_D\\ \text{via cell proliferation}}}$$

$$
\begin{aligned}
& \underbrace{-\frac{R_D}{R_D+C_D}R_{T_D}\mathscr{D}_{\mathscr{D}}(E,\phi_D)}_{\substack{\text{Loss of } R_D \\ \text{via cell death}}} \\
\frac{dC_D}{dt} &= + \underbrace{k_f L R_D}_{\text{IL6 binding to } R_D} - \underbrace{k_r C_D}_{\substack{\text{IL6 dissociation} \\ \text{from } R_D}} - \underbrace{k_p C_D}_{\text{Internalization}} - \underbrace{\frac{C_D}{R_D+C_D}R_{T_D}\mathscr{D}_{\mathscr{D}}(D,\phi_D)}_{\substack{\text{Loss of } C_D \\ \text{via cell death}}} \\
\frac{dX}{dt} &= + \underbrace{k_{12}^C X_s - k_{21}^C X}_{\text{Pharmacokinetics}}
\end{aligned}
$$

where, X_s denotes the concentration of free cisplatin in circulating blood.

Pharmacokinetics of cisplatin

To estimate the pharmacokinetic parameters of cisplatin we use the analytic solution of the PK-model with i.p. injection introduce in [1] and given by:

$$
X_s(t) = X_p(t_0)\left(A_p e^{-\alpha(t-t_0)} + B_p e^{-\beta(t-t_0)}\right), t \geq t_0 \tag{S42}
$$

where,

$$
\begin{aligned}
\alpha &= \frac{(k_{12}^C + k_{21}^C + k_{el}^C) + \sqrt{(k_{12}^C + k_{21}^C + k_{el}^C)^2 - 4k_{21}^C k_{el}^C}}{2} \\
\beta &= \frac{(k_{12}^C + k_{21}^C + k_{el}^C) - \sqrt{(k_{12}^C + k_{21}^C + k_{el}^C)^2 - 4k_{21}^C k_{el}^C}}{2} \\
A_p &= \frac{k_{21}^C}{\beta - \alpha} \\
B_p &= \frac{k_{21}^C}{\alpha - \beta}
\end{aligned}
$$

where k_{12}^C and k_{21}^C are the distribution rate constants between the systemic central compartment (X_s) and peripheral compartment (X_p). Moreover, k_{el}^C is the elimination rate from central compartment. In order to estimate the pharmacokinetic parameters, we used the data given in [8]. Figure S3 shows the best-fit of the pharmacokinetic model to the data. Variables related to cisplatin-therapy model and the estimated parameter values are listed in Tables S7 and S8.

Developing Equations for TCZ therapy Model

As an anti-IL-6R antibody, TCZ binds to IL-6R on tumor cells and inhibits the formation of IL-6- IL-6R complex molecules. All equations related to treatment with anti-IL-6R antibody (i.e., $\frac{dI}{dt}$, $\frac{dC_S^I}{dt}$, $\frac{dC_E^I}{dt}$ and $\frac{dC_D^I}{dt}$) are described in [1]. The Full TCZ therapy model is given by:

$$\frac{dH}{dt} = \underbrace{\alpha_H \phi_{H_{A2}}^{n_H} H}_{\substack{\text{Activated VEGFR2-mediated} \\ \text{proliferation}}} - \underbrace{\frac{\delta_H}{1+\beta_H B_H} H}_{\substack{\text{Bcl-2-mediated} \\ \text{apoptosis}}}$$

$$\frac{dS}{dt} = \underbrace{\alpha_S P_S(S,\phi_S) S \mathcal{H}(N-N_p)}_{\text{Stem cell self-renewal}} - \underbrace{\frac{\delta_S}{1+\gamma_S \phi_S} S[1+\mathcal{H}(N_d-N)]}_{\substack{\text{IL-6 \& Bcl-2 mediated} \\ \text{apoptosis}}}$$

$$\frac{dE}{dt} = \underbrace{A_{in}\alpha_S \left[1-P_S(S,\phi_S)\right] S \mathcal{H}(N-N_p)}_{\substack{\text{Amplified} \\ \text{stem cell differentiation}}} - \underbrace{\alpha_E E \mathcal{H}(N-N_p)}_{\substack{\text{Progenitor cell} \\ \text{differentiation}}}$$
$$\underbrace{-\frac{\delta_E}{1+\gamma_E \phi_E} E[1+\mathcal{H}(N_d-N)]}_{\substack{\text{IL-6 \& Bcl-2 mediated} \\ \text{apoptosis}}}$$

$$\frac{dD}{dt} = \underbrace{2\alpha_E E \mathcal{H}(N-N_p)}_{\substack{\text{progenitor cell} \\ \text{differentiation}}} \underbrace{-\frac{\delta_D}{1+\gamma_D \phi_D} D[1+\mathcal{H}(N_d-N)]}_{\substack{\text{IL-6 \& Bcl-2 mediated} \\ \text{apoptosis}}}$$

$$\frac{dL}{dt} = -\underbrace{k_f L R_S}_{\substack{\text{IL-6 binding to} \\ \text{stem cells}}} + \underbrace{k_r C_S}_{\substack{\text{IL6 dissociation} \\ \text{from stem cells}}} - \underbrace{k_f L R_E}_{\substack{\text{IL-6 binding to} \\ \text{progenitor cells}}} + \underbrace{k_r C_E}_{\substack{\text{IL-6 dissociation} \\ \text{from progenitor cells}}}$$
$$- \underbrace{k_f L R_D}_{\substack{\text{IL-6 binding to} \\ \text{differentiated cells}}} + \underbrace{k_r C_D}_{\substack{\text{IL-6 dissociation} \\ \text{from differentiated cells}}} - \underbrace{\lambda_L L}_{\text{IL-6 natural decay}}$$
$$+ \underbrace{\rho_T (S+E+D)}_{\substack{\text{IL-6 Production} \\ \text{by tumor cells}}} + \underbrace{\rho_H \phi_{H_{A2}}^{n_L} H}_{\substack{\text{Bcl-2-mediated} \\ \text{IL-6 production} \\ \text{by ECs}}}$$

$$\frac{dI}{dt} = -\underbrace{k_f^I I R_S}_{\substack{\text{Anti-IL6R binding to} \\ \text{stem cells}}} + \underbrace{k_r^I C_S^I}_{\substack{\text{Ani-IL6R dissociation} \\ \text{from stem cells}}} - \underbrace{k_f^I I R_E}_{\substack{\text{Anti-IL6R binding to} \\ \text{progenitor cells}}}$$
$$+ \underbrace{k_r^I C_E^I}_{\substack{\text{Anti-IL6R dissociation} \\ \text{from progenitor cells}}} - \underbrace{k_f^I I R_D}_{\substack{\text{Anti-IL6R binding to} \\ \text{differentiated cells}}} + \underbrace{k_r^I C_D^I}_{\substack{\text{IL6 dissociation} \\ \text{from differentiated cells}}}$$

$$
\begin{aligned}
&+ \underbrace{k_{12}I_s - k_{21}I}_{\text{Pharmacokinetics}} \\
\frac{dR_S}{dt} &= - \underbrace{k_f L R_S}_{\substack{\text{IL-6 binding to}\\ \text{stem cells}}} + \underbrace{k_r C_S}_{\substack{\text{IL-6 dissociation}\\ \text{from stem cells}}} + \underbrace{k_p C_S}_{\text{Recycling}} - \underbrace{k_f^I I R_S}_{\substack{\text{Anti-IL6R binding to}\\ \text{IL-6R}}} \\
&+ \underbrace{k_r^I C_S^I}_{\substack{\text{Anti-IL-6R dissociation}\\ \text{from stem cells}}} + \underbrace{R_{T_S}\mathscr{P}_{\mathscr{S}}(S,\phi_S)}_{\substack{\text{Generation of new } R_S\\ \text{via cell proliferation}}} - \underbrace{\frac{R_S}{R_S+C_S+C_S^I}R_{T_S}\mathscr{D}_{\mathscr{S}}(S,\phi_S)}_{\substack{\text{Loss of } R_S\\ \text{via cell death}}} \\
\frac{dC_S^I}{dt} &= + \underbrace{k_f^I I R_S}_{\substack{\text{Anti-IL6R binding to}\\ \text{IL-6R}}} - \underbrace{k_r^I C_S^I}_{\substack{\text{Ani-IL6R dissociation}\\ \text{from stem cells}}} - \underbrace{\frac{C_S^I}{R_S+C_S+C_S^I}R_{T_S}\mathscr{D}_{\mathscr{S}}(S,\phi_S)}_{\substack{\text{Loss of } C_S^I\\ \text{via cell death}}} \\
\frac{dC_S}{dt} &= + \underbrace{k_f L R_S}_{\text{IL6 binding to } R_S} - \underbrace{k_r C_S}_{\substack{\text{IL6 dissociation}\\ \text{from } R_S}} - \underbrace{k_p C_S}_{\text{Internalization}} - \underbrace{\frac{C_S}{R_S+C_S+C_S^I}R_{T_S}\mathscr{D}_{\mathscr{S}}(S,\phi_S)}_{\substack{\text{Loss of } C_S\\ \text{via cell death}}} \\
\frac{dR_E}{dt} &= - \underbrace{k_f L R_E}_{\substack{\text{IL-6 binding to}\\ \text{progenitor cells}}} + \underbrace{k_r C_E}_{\substack{\text{IL-6 dissociation}\\ \text{from progenitor cells}}} + \underbrace{k_p C_E}_{\text{Recycling}} - \underbrace{k_f^I I R_E}_{\substack{\text{Anti-IL6R binding to}\\ \text{IL-6R}}} \\
&+ \underbrace{k_r^I C_E^I}_{\substack{\text{Anti-IL-6R dissociation}\\ \text{from progenitor cells}}} + \underbrace{R_{T_E}\mathscr{P}_{\mathscr{E}}(E,\phi_E)}_{\substack{\text{Generation of new } R_E\\ \text{via cell proliferation}}} - \underbrace{\frac{R_E}{R_E+C_E+C_E^I}R_{T_E}\mathscr{D}_{\mathscr{E}}(E,\phi_E)}_{\substack{\text{Loss of } R_E\\ \text{via cell death}}} \\
\frac{dC_E^I}{dt} &= + \underbrace{k_f^I I R_E}_{\substack{\text{Anti-IL6R binding to}\\ \text{IL-6R}}} - \underbrace{k_r^I C_E^I}_{\substack{\text{Ani-IL6R dissociation}\\ \text{from progenitor cells}}} - \underbrace{\frac{C_E^I}{R_E+C_E+C_E^I}R_{T_E}\mathscr{D}_{\mathscr{E}}(E,\phi_E)}_{\substack{\text{Loss of } C_E^I\\ \text{via cell death}}} \\
\frac{dC_E}{dt} &= + \underbrace{k_f L R_E}_{\text{IL6 binding to } R_E} - \underbrace{k_r C_E}_{\substack{\text{IL6 dissociation}\\ \text{from } R_E}} - \underbrace{k_p C_E}_{\text{Internalization}} - \underbrace{\frac{C_E}{R_E+C_E+C_E^I}R_{T_E}\mathscr{D}_{\mathscr{E}}(E,\phi_E)}_{\substack{\text{Loss of } C_E\\ \text{via cell death}}} \\
\frac{dR_D}{dt} &= - \underbrace{k_f L R_D}_{\substack{\text{IL-6 binding to}\\ \text{differentiated cells}}} + \underbrace{k_r C_D}_{\substack{\text{IL-6 dissociation}\\ \text{from differentiated cells}}} + \underbrace{k_p C_D}_{\text{Recycling}} - \underbrace{k_f^I I R_D}_{\substack{\text{Anti-IL6R binding to}\\ \text{IL-6R}}} \\
&+ \underbrace{k_r^I C_D^I}_{\substack{\text{Anti-IL-6R dissociation}\\ \text{from differentiated cells}}} + \underbrace{R_{T_D}\mathscr{P}_{\mathscr{D}}(E,\phi_D)}_{\substack{\text{Generation of new } R_D\\ \text{via cell proliferation}}} - \underbrace{\frac{R_D}{R_D+C_D+C_D^I}R_{T_D}\mathscr{D}_{\mathscr{D}}(E,\phi_D)}_{\substack{\text{Loss of } R_D\\ \text{via cell death}}} \\
\frac{dC_D^I}{dt} &= + \underbrace{k_f^I I R_D}_{\substack{\text{Anti- nding to}\\ \text{IL-6R}}} - \underbrace{k_r^I C_D^I}_{\substack{\text{Ani-IL6R dissociation}\\ \text{from differentiated cells}}} - \underbrace{\frac{C_D^I}{R_D+C_D+C_D^I}R_{T_D}\mathscr{D}_{\mathscr{D}}(D,\phi_D)}_{\substack{\text{Loss of } C_D^I\\ \text{via cell death}}}
\end{aligned}
$$

$$
\begin{aligned}
\frac{dC_D}{dt} &= + \underbrace{k_f L R_D}_{\text{IL6 binding to } R_D} - \underbrace{k_r C_D}_{\substack{\text{IL6 dissociation} \\ \text{from } R_D}} - \underbrace{k_p C_D}_{\text{Internalization}} \\
&\quad \underbrace{- \frac{C_D}{R_D + C_D + C_D^I} R_{T_D} \mathscr{D}_{\mathscr{D}}(D, \phi_D)}_{\substack{\text{Loss of } C_D \\ \text{via cell death}}} \\
\frac{dA}{dt} &= \underbrace{-k_{H1}^f R_{H_{A1}} A + k_{H1}^r C_{H_{A1}} - k_{H2}^f R_{H_{A2}} A + k_{H2}^r C_{H_{A2}}}_{\text{reaction with VEGFR1/2 on endothelial cells}} \\
&\quad - \underbrace{\lambda_A A}_{\substack{\text{natural} \\ \text{decay}}} + \underbrace{\alpha_A \frac{B_H}{1 + \beta_A B_H} H}_{\substack{\text{Bcl-2-mediated production} \\ \text{by endothelial cells}}} + \underbrace{\frac{\nu_A}{1 + e^{-\kappa_A (N_h - N)}} (S + E + D)}_{\substack{\text{hypoxia-mediated VEGF} \\ \text{production by stem/bulk cells}}} \\
\frac{dC_{H_{A1}}}{dt} &= \underbrace{k_{H1}^f R_{H_{A1}} A - k_{H1}^r C_{H_{A1}} - k_{H1}^p C_{H_{A1}}}_{\substack{\text{VEGFR1 activation by VEGF} \\ \text{on endothelial cells}}} - \underbrace{C_{H_{A1}} \frac{\delta_H}{1 + \beta_H B_H}}_{\substack{\text{loss due to} \\ \text{endothelial cell apoptosis}}} \\
\frac{dC_{H_{A2}}}{dt} &= \underbrace{k_{H2}^f R_{H_{A2}} A - k_{H2}^r C_{H_{A2}} - k_{H2}^p C_{H_{A2}}}_{\substack{\text{VEGFR2 activation by VEGF} \\ \text{on endothelial cells}}} - \underbrace{C_{H_{A2}} \frac{\delta_H}{1 + \beta_H B_H}}_{\substack{\text{loss due to} \\ \text{endothelial cell apoptosis}}} \\
\frac{dB_H}{dt} &= \underbrace{\chi_H}_{\substack{\text{Constitutive} \\ \text{expression} \\ \text{by ECs}}} + \underbrace{\eta_H \frac{\phi_{H_{A2}}^{n_B}}{\omega_H^{n_B} + \phi_{H_{A2}}^{n_B}}}_{\substack{\text{Activated VEGFR2-} \\ \text{mediated production} \\ \text{by ECs}}} - \underbrace{\delta_B B_H}_{\substack{\text{natural} \\ \text{decay}}}
\end{aligned}
$$

It is worth mentioning that the following equations for TCZ therapy model satisfy:

$$
\begin{aligned}
R_S &= R_{T_S} S - C_S - C_S^I \\
R_E &= R_{T_E} E - C_E - C_E^I \\
R_D &= R_{T_D} D - C_D - C_D^I
\end{aligned}
$$

Pre-treatment experimental data

To begin to evaluate the role of endothelial cell-secreted IL-6 on the tumorigenic potential and survival of primary human HNSCC CSCs, Krishnamurthy et al. [9] silenced the IL-6 secretion

in endothelial cells and used these cells to generate tumor xenografts with a humanized vasculature. Briefly, immediately after surgical removal of the primary tumor from patients with HNSCC, they sorted and seeded 1'000 HNSCC CSCs ($ALDH^{HIGH}CD44^{HIGH}$ cells) into IL-6 +/+ immunodeficient mice along with 5×10^5 either IL-6-silenced endothelial cells (HDMEC-shRNA-IL-6) or endothelial cells transduced with empty lentiviral vectors (HDMEC-shRNA-C) in poly(L-lactic) acid biodegradable scaffolds. Bilateral scaffolds were implanted subcutaneously in the dorsum of each mouse. Tumor volumes were calculated and recorded over 81 days after implantation. Figure S2 shows the relevant data directly taken from [9]. The blue circles show the volume of xenograft tumors vascularized with HDMEC-shRNA-C and the red circles show the volume of the xenograft tumors vascularized with control HDMEC-shRNA-IL-6 over days after implantation. The blue and red dots depict the average tumor volume vascularized with HDMEC-shRNA-C and HDMEC-shRNA-IL-6, respectively. Moreover, they evaluated the percentage of CSCs in those xenograft tumors and reported that ablation of EC-IL-6 within the tumor microenvironment reduced the fraction of CSCs in tumor (right panels in Fig. S2-A and B).

Pre-treatment experimental data

To begin to evaluate the role of endothelial cell-secreted IL-6 on the tumorigenic potential and survival of primary human HNSCC CSCs, Krishnamurthy et al. [9] silenced the IL-6 secretion in endothelial cells and used these cells to generate tumor xenografts with a humanized vasculature. Briefly, immediately after surgical removal of the primary tumor from patients with HNSCC, they sorted and seeded 1'000 HNSCC CSCs ($ALDH^{HIGH}CD44^{HIGH}$ cells) into IL-6 +/+ immunodeficient mice along with 5×10^5 either IL-6-silenced endothelial cells (HDMEC-shRNA-IL-6) or endothelial cells transduced with empty lentiviral vectors (HDMEC-shRNA-C) in poly(L-lactic) acid biodegradable scaffolds. Bilateral scaffolds were implanted subcutaneously in the dorsum of each mouse. Tumor volumes were calculated and recorded over 81 days after implantation. Figure S2 shows the relevant data directly taken from [9]. The blue circles show the volume of xenograft tumors vascularized with HDMEC-shRNA-C and the red circles show the volume of the xenograft tumors vascularized with control HDMEC-shRNA-IL-6 over days after implantation. The blue

and red dots depict the average tumor volume vascularized with HDMEC-shRNA-C and HDMEC-shRNA-IL-6, respectively. Moreover, they evaluated the percentage of CSCs in those xenograft tumors and reported that ablation of EC-IL-6 within the tumor microenvironment reduced the fraction of CSCs in tumor (right panels in Fig. S2-A and B).

Estimating baseline parameter values of pre-treatment model

Initially, we fit the mathematical model to the mice data for primary human HNSCC CSCs implanted without human endothelial cells in [3] in order to estimate the baseline parameter values associated with CSC and IL-6 modules that we could not obtain in the current literature (transit-amplifying factor (A_{in}), number of stem cells for which the probability of symmetric self-renewal is halfway between the maximum and minimum value (P_{N_s}), IL-6R recycling rate on tumor cell surface (k_p), and IL-6-induced death modification parameter (γ_i) and modulation parameter that adjusts the effects of IL-6 on the probability of CSC self-renew (μ). We use 24 data points for tumor volume over time (day 50 through day 121) to estimate the parameters. CSC% at day 30 is predicted using the estimated parameter (Figure 5 in [1]). A list of parameter values found from the literature are tabulated in Tables S3 and S4. The baseline values for the remaining parameters are estimated by fitting the pre-treatment EC-TC model to the control data. We use *Monte Carlo parameter sweep method* [3] to minimize the weighted least squares by comparing the average tumor volume extracted from the data and the tumor volume predicted by the pre-treatment EC-TC model, over days after implantation. Fig. S2-A depicts the best-fit to the control data (black line). The estimated best-fit parameter values are tabulated in Table S5 in Supplementary Material.

Recall that in the experiment described in Fig. S2, $\text{ALDH}^{\text{HIGH}}\text{CD44}^{\text{HIGH}}$ cells were sorted from "primary" human HNSCC tumor and implanted in mice along with endothelial cells to study the impacts of endothelial cell-secreted IL-6 on tumor initiation and tumorigenic properties of CSCs. Primary cells are isolated directly from human or animal tissue and are immediately placed in an artificial environment whereas cell lines have been continually passaged over a long period of time and have acquired homogenous genotypic and phenotypic characteristics. Immortalized or continuous cell lines have acquired the ability to proliferate indefinitely. Moreover, despite the fact

that cell lines have lost the true characteristics of the original tissue from which they were isolated, they are widely used in lab experiments as they are easy to handle. In contrast, primary cells usually are believed to be more biologically relevant tools than cell lines but they have a limited lifespan, slow proliferation and are not well characterized making them hard to maintain. Therefore, since primary cells and cell lines show different behavior, we, firstly, need to find the baseline parameter values for each aforementioned cell lines. Secondly, we add equations related to treatment to the current model and use those obtained baseline parameter values to predict the rate of tumor growth post treatment with TCZ and/or cisplatin and with the combination therapy of TCZ and cisplatin. Finally, we use our model to make suggestions/predictions for the most optimized dosing/scheduling combination of cisplatin and TCZ.

Endothelial cell-secreted IL-6 enhances primary HNSCC tumor growth

To evaluate the impacts of EC-secreted IL-6 on the tumorigenic potential of CSCs, xenograft tumors were generated in immunodeficient mice by using HDMEC-shRNA-C and HDMEC-shRNA-IL-6R and it was shown that silencing EC secreted IL-6 could significantly decrease the tumor growth rate and the percentage of CSCs in primary tumors (Figure S2). In order to calibrate and test the abilities of the proposed pre-treatment model, we first fit it to the control data related to HDMEC-shRNA-C (Figure S2-A) and estimated the unknown parameter values. There are four parameters from the EC-TC crosstalk model (i.e., EC division rate (α_H), and Bcl-2-mediated death modulation parameter (β_H), IL-6 section rate by ECs (ρ_H) and modulation parameter that adjusts the rate of Bcl-2-mediated VEGF secretion by ECs (β_A)) are estimated to match this experimental system described above. The estimated parameter values are listed in Table S5. We also used the estimated baseline parameter values to predict the percentage of CSC% at day 30 after implantation and compared it to the CSC% (Figure S2-A). Then after, we decreased the secretion rate of IL-6 by ECs to a very low level and used it to predicted tumor volume growth dynamics over time. However, the numerical simulations suggest (data is not shown) that some of the parameters that are influenced by IL-6 should be also altered. As it is discussed in [1], disturbance of IL-6 secretion can potentially change the amplifying factor and the probability of CSC self-renewal. Therefore,

in order to estimate the new altered values of related parameters (n, A_{in} and P_{N_s}), we fit the pre-treatment model to HDMEC-shRNA-IL-6 data when the rate of EC-IL-6 secretion, ρ_H, is much smaller as compared to control case (Figure S2-B). Model predictions for both HDMEC-shRNA-IL-6 and HDMEC-shRNA-C data indicate that the proposed model is capable of making reliable predictions of tumor growth.

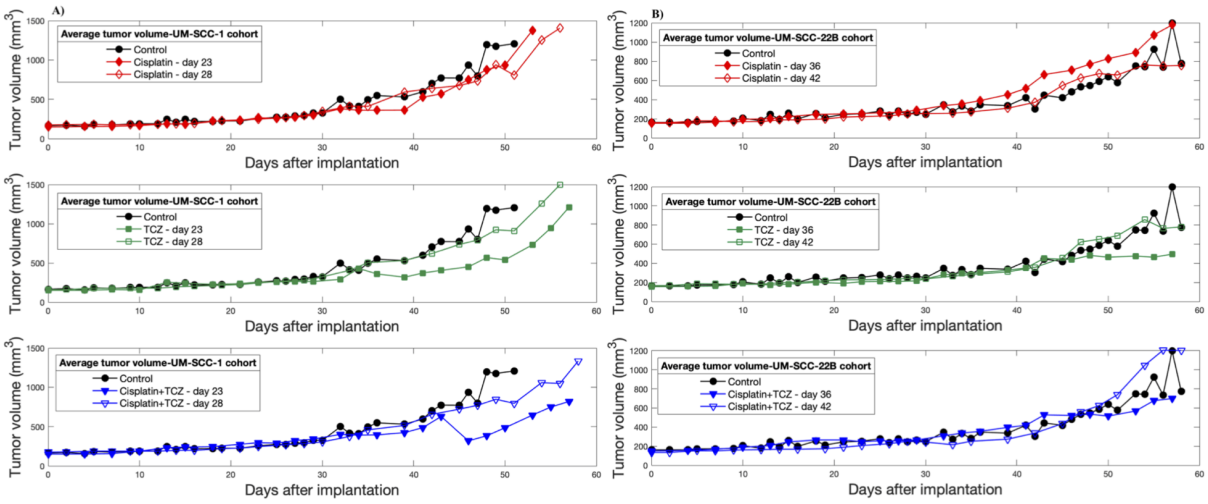

FIGURE S1. Effects of TCZ and/or cisplatin on tumor growth in the pre-clinical experimental setup of UM-SCC-1 and UM-SCC-22B cohort.

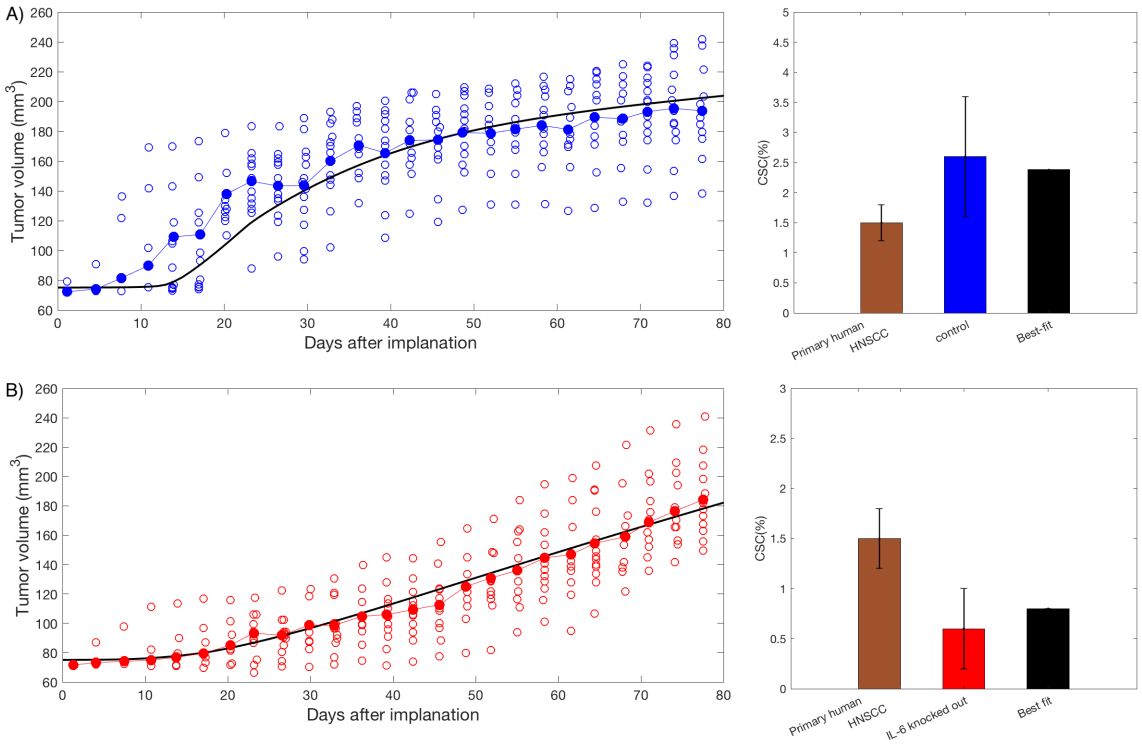

FIGURE S2. The best-fit of the pre-treatment EC-TC model to EC-IL-6-silent and EC-IL-6-control data: (A) 1'000 primary human $ALDH^{HIGH}CD44^{HIGH}$ cells along with HDMEC-shRNA-C cells were seeded in 13 mice; blue circles represent the individual tumor volumes over time, blue dots represent the average tumor volume at each time point and the black solid line shows the tumor volumes predicted by the pre-treatment EC-TC model. Right panel shows the percentage of ($ALDH^{HIGH}CD44^{HIGH}$) cells; the orange bar shows the CSC% in primary human HNSCC; the blue bar shows the CSC% in xenograft tumor vascularized with HDMEC-shRNA-C; and the red bar shows the CSC% predicted by the pre-treatment EC-TC model in the xenograft tumor vascularized with HDMEC-shRNA-C at day 30 after implantation. (B) 1'000 primary human $ALDH^{HIGH}CD44^{HIGH}$ cells along with HDMEC-shRNA-IL-6 cells were seeded in 13 mice; red circles represent the individual tumor volumes over time, red dots represent the average tumor volume at each time point and the black solid line shows the tumor volumes predicted by the pre-treatment EC-TC model. Right panel depicts the percentage of ($ALDH^{HIGH}CD44^{HIGH}$) cells; the orange bar, the red and the black bars shows the CSC% in primary human HNSCC, the CSC% in xenograft tumor vascularized with HDMEC-shRNA-C, and the CSC% predicted by the pre-treatment EC-TC model in the xenograft tumor vascularized with HDMEC-shRNA-Il-6 at day 30 after implantation, respectively.

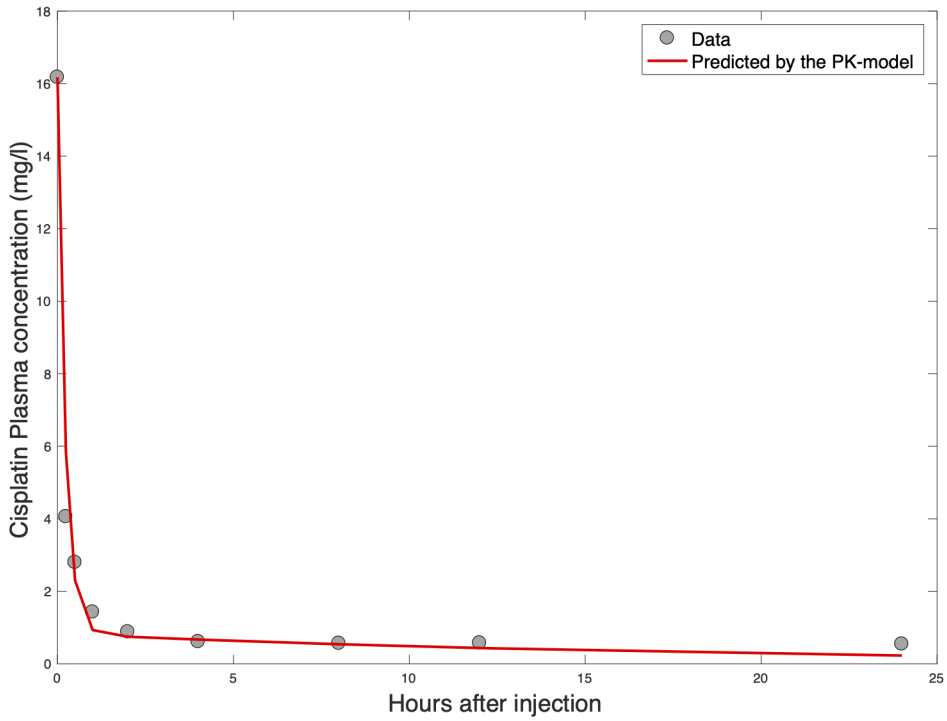

FIGURE S3. Time profiles of plasma cisplatin concentration given in [8]. The gray points depict Pt concentration in the plasma versus time after a single intravenous injection of cisplatin in rats. Data are presented as mean ± SD (n = 12) and the solid red line shows the model prediction of cisplatin elimination from plasma.

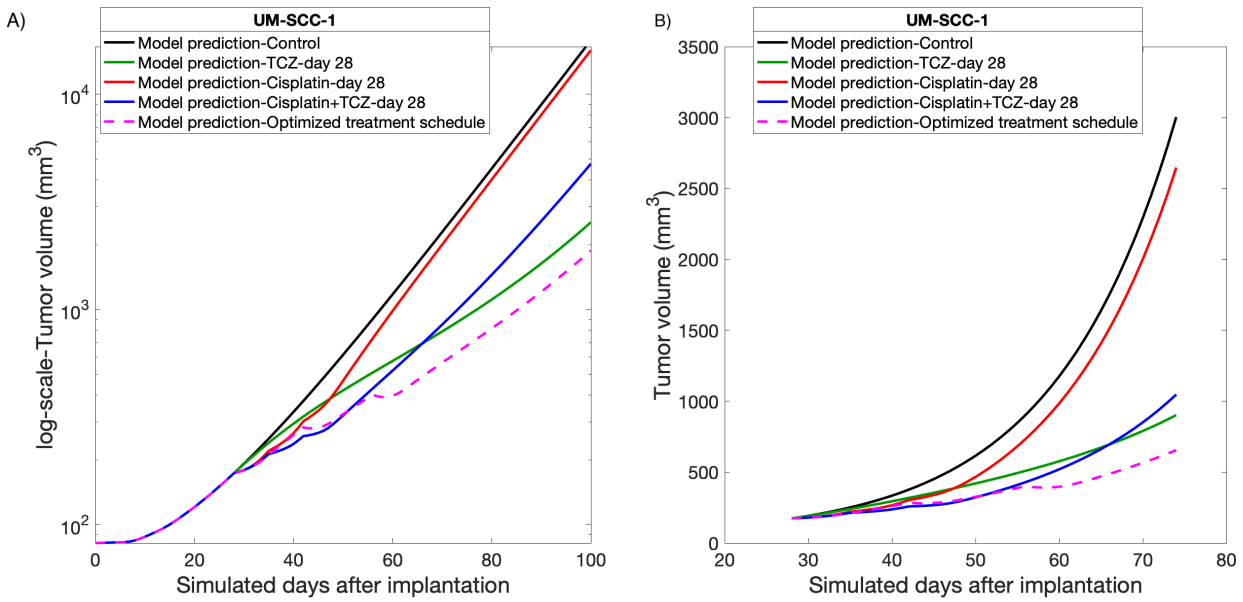

FIGURE S4. Simulation results for single therapy and combination therapy for longer times. (A) The non-optimal combination therapy schedule given experimentally is initially more effective at tumor reduction than either TCZ or cisplatin alone. However, over time TCZ alone leads to a better result than non-optimal combination therapy. Simulating the optimal dosing schedule predicted by the model and comparing it to the results obtained from the experiment shows that the predicted optimal dosing schedule is better than either therapy alone and is also more effective than the co-treatment strategy used experimentally. (B) Closer look at tumor growth shows that after day 67, TCZ therapy leads to a better result than co-therapy strategy used experimentally.

TABLE S1. Statistical Modeling of Tumor Size Change

UM-SCC-1 Coefficients:	Value	Std. Error	p-value
Days	0.0417	0.0016	< 0.0001
Days $\times$ cisplatin	-0.0064	0.0016	< 0.0001
Days $\times$ tocilizumab	-0.0091	0.0017	< 0.0001
UM-SCC-22B Coefficients:	Value	Std. Error	p-value
Days	0.0446	0.0019	< 0.0001
Days $\times$ cisplatin	0.0009	0.0021	0.6758
Days $\times$ tocilizumab	-0.0062	0.0021	0.0033

TABLE S2. Description of Variables of EC-TC Cross-Talk Model

Variables	Description	Units
H	Endothelial cell number	#
S	Cancer stem cell number	#
E	Progenitor cell number	#
D	Differentiated cell number	#
A	Amount of free VEGF	fmol
$R_{H_{A1}}$	Number of free VEGFR1 on endothelial cells	fmol
$R_{H_{A2}}$	Number of free VEGFR2 on endothelial cells	fmol
$C_{H_{A1}}$	VEGF-VEGFR1 complexes on endothelial cells	fmol
$C_{H_{A2}}$	VEGF-VEGFR2 complexes on endothelial cells	fmol
L	IL-6 secreted by endothelial & tumor (stem/non-stem) cells	fmol
R_S	IL-6R on tumor stem cells	fmol
R_E	IL-6R on tumor progenitor cells	fmol
R_D	IL-6R on tumor differentiated cells	fmol
C_S	IL-6–IL-6R complex on tumor stem cell	fmol
C_E	IL-6–IL-6R complex on tumor progenitor cell	fmol
C_D	IL-6–IL-6R complex on tumor differentiated cell	fmol
B_H	Bcl-2 mRNA expression level per endothelial cell	dimensionless

TABLE S3. Parameter values taken from the literature and their sources.
* Vol_T is the volume of the tumor in μl and is equal to (volume of 1 million ECs)× H+ (volume of 1 million TCs) × (S+E+D), where, the volume of 1 EC is $2.2 \times 10^{-6} \mu l$ [10] and 1 TC is $1 \times 10^{-6} \mu l$ [11].

Parameter	**Value**	**Units**	**Source**
α_S	0.6	day^{-1}	[12, 13]
α_E	$\frac{log(2)}{1.04}$	day^{-1}	[12, 13]
$P^*_{S_{min}}$	0.014	dimensionless	[14]
$P_{S_{max}}$	0.90	dimensionless	[14]
k_f	2.35	$\text{fmol}^{-1}\text{day}^{-1}$	[15]
k_r	2.24	day^{-1}	[16, 15]
λ_L	0.4152	day^{-1}	[17]
ρ_T	7×10^{-7}	$\text{fmol}^{-1}\text{day}^{-1}$per cell	[18, 19, 20]
R_{T_S}	1.66×10^{-6}	fmol^{-1}per cell	[21, 22, 23, 24]
R_{T_E}	$\frac{1}{8} R_{T_S}$	fmol^{-1}per cell	[9]
R_{T_D}	$\frac{1}{8} R_{T_S}$	fmol^{-1}per cell	[9]
k^f_{H1}	$11.4048/\text{Vol}^*_T$	fmol^{-1} day^{-1}	[25, 26]
k^r_{H1}	86.4	day^{-1}	[27]
k^p_{H1}	24.1920	day^{-1}	[27]
k^f_{H2}	$10.0757/\text{Vol}^*_T$	fmol^{-1} day^{-1}	[11, 25]
k^r_{H2}	86.4	day^{-1}	[27]
k^p_{H2}	24.1920	day^{-1}	[27]
$R^t_{H_{A1}}$	6.63e-5	fmol per cell	[28]
$R^t_{H_{A2}}$	1.92e-4	fmol per cell	[28]
λ_A	16.6355	day^{-1}	[29]
δ_B	6.6542	day^{-1}	[30]

TABLE S4. Continuation of Table S3: Parameter values taken from literature and their sources

Parameter	**Estimated Value**	**Units**	**Source**
δ_H	0.09	per day	[2]
N_p	5.5	mmHg	[2]
δ_S	0.0126	day^{-1}	[1]
N_d	1	mmHg	[2]
γ_S	2.38	dimensionless	[1]
δ_E	0.0125	day^{-1}	[1]
γ_E	2.38	dimensionless	[1]
δ_D	0.5	day^{-1}	[1]
μ_S	0.018	dimensionless	[1]
γ_D	2.38	dimensionless	[1]
k_p	24.95	day^{-1}	[1]
P_{N_s}	7.62e+05	dimensionless	[1]
α_A	6.25e-07	fmol cell^{-1} day^{-1}	[2]
ν_A	5e-4	fmol cell^{-1} day^{-1}	[2]
κ_A	2	dimensionless	[2]
N_h	10	mmHg	[2]
χ_H	6.6542	per day	[2]
η_H	1063	per day	[2]
ω_H	0.3341	dimensionless	[2]
n_B	5	dimensionless	[2]
σ_N	1.087	mmHg	[2]

TABLE S5. Estimated parameter values for the pre-treatment EC-TC model using primary human HNSCC data directly taken from [9] (Figure S2)

Parameter	**Estimated Value**	**Units**	**Source**
α_H	0.5	per day	Estimated
β_H	600	dimensionless	Estimated
ρ_H	0.0052	$\text{fmol}^{-1}\text{day}^{-1}\text{cell}^{-1}$	Estimated
β_A	0.65	dimensionless	Estimated
n_L	3	dimensionless	Assumed
A_{in}	4	dimensionless	Assumed
n	9	dimensionless	Assumed
n_H	0.5	dimensionless	Assumed

TABLE S6. Estimated parameter values for the pre-treatment EC-TC model using control UM-SCC-1 and UM-SCC-22B cohort data

Parameter	**Estimated Value (UM-SCC-1)**	**Estimated Value (UM-SCC-22B)**	**Units**
α_E	0.016	0.016	dimensionless (Assumed)
n	7	10	dimensionless
μ_S	0.10	0.095	dimensionless
A_{in}	10	4	dimensionless
P_{N_s}	2.1+05	3.7e+05	dimensionless
n_L	0.8	0.8	dimensionless (Assumed)

TABLE S7. Variables related to cisplatin-therapy model

Variable	**Description**	**Units**
X	Free cisplatin in tumor	fmol
X_s	Free cisplatin in systemic circulation	fmol
X_p	Free cisplatin in peripheral compartment	fmol

TABLE S8. Estimated pharmacokinetic parameters of cisplatin

Parameters	**Values**	**Units**	**Reference**
k_{12}^C	84	day^{-1}	Estimated
k_{21}^C	7	day^{-1}	Estimated
k_{el}^C	20	day^{-1}	Estimated

TABLE S9. Baseline parameter values for the cisplatin-therapy model using data related to cisplatin therapy for UM-SCC-1 and UM-SCC-22B cohorts.

Parameter	**UM-SCC-1**	**UM-SCC-22B**	**Units**	**Source**
Π_S	0.59	0.081	dimensionless	Estimated
Π_E	1.98	0.071	dimensionless	Estimated
Π_D	3.5	0.023	dimensionless	Estimated
K_S	1e+32	1e+09	fmol	Assumed
K_M^S	8.3e+05	8.65e+05	fmol	[7]
K_M^E	8.3e+05	8.65e+05	fmol	[7]
K_M^D	8.3e+05	8.65e+05	fmol	[7]

References

[1] Nazari F, Pearson AT, Nör JE, Jackson TL. A mathematical model for IL-6-mediated, stem cell driven tumor growth and targeted treatment. PLoS computational biology. 2018;14(1):e1005920.

[2] Jain HV, Jackson T. Mathematical Modeling of Cellular Cross-Talk Between Endothelial and Tumor Cells Highlights Counterintuitive Effects of VEGF-Targeted Therapies. Bulletin of Mathematical Biology. 2017;.

[3] Cowan G. Statistical data analysis. Oxford University Press; 1998.

[4] Kaneko T, Zhang Z, Mantellini MG, Karl E, Zeitlin B, Verhaegen M, et al. Bcl-2 orchestrates a cross-talk between endothelial and tumor cells that promotes tumor growth. Cancer research. 2007;67(20):9685–9693.

[5] Neiva KG, Zhang Z, Miyazawa M, Warner KA, Karl E, Nör JE. Cross talk initiated by endothelial cells enhances migration and inhibits anoikis of squamous cell carcinoma cells through STAT3/Akt/ERK signaling. Neoplasia. 2009;11(6):583–IN14.

[6] Tarquinio SB, Zhang Z, Neiva KG, Polverini PJ, Nör JE. Endothelial cell Bcl-2 and lymph node metastasis in patients with oral squamous cell carcinoma. Journal of Oral Pathology & Medicine. 2012;41(2):124–130.

[7] Nör C, Zhang Z, Warner KA, Bernardi L, Visioli F, Helman JI, et al. Cisplatin induces Bmi-1 and enhances the stem cell fraction in head and neck cancer. Neoplasia. 2014;16(2):137–W8.

[8] Ling X, Shen Y, Sun R, Zhang M, Li C, Mao J, et al. Tumor-targeting delivery of hyaluronic acid–platinum (iv) nanoconjugate to reduce toxicity and improve survival. Polymer Chemistry. 2015;6(9):1541–1552.

[9] Krishnamurthy S, Warner KA, Dong Z, Imai A, Nör C, Ward BB, et al. Endothelial Interleukin-6 Defines the Tumorigenic Potential of Primary Human Cancer Stem Cells. Stem Cells. 2014;32(11):2845–2857.

[10] King J, Hamil T, Creighton J, Wu S, Bhat P, McDonald F, et al. Structural and functional characteristics of lung macro-and microvascular endothelial cell phenotypes. Microvascular research. 2004;67(2):139–151.

[11] Cunningham SA, Tran TM, Arrate MP, Brock TA. Characterization of Vascular Endothelial Cell Growth Factor Interactions with the Kinase Insert Domain-containing Receptor Tyrosine Kinase A REAL TIME KINETIC STUDY. Journal of Biological Chemistry. 1999;274(26):18421–18427.

[12] Driessens G, Beck B, Caauwe A, Simons BD, Blanpain C. Defining the mode of tumour growth by clonal analysis. Nature. 2012;488(7412):527–530.

[13] Gao X, McDonald JT, Hlatky L, Enderling H. Acute and fractionated irradiation differentially modulate glioma stem cell division kinetics. Cancer research. 2013;73(5):1481–1490.

[14] Weekes SL, Barker B, Bober S, Cisneros K, Cline J, Thompson A, et al. A multicompartment mathematical model of cancer stem cell-driven tumor growth dynamics. Bulletin of mathematical biology. 2014;76(7):1762–1782.

[15] Özbek S, Grötzinger J, Krebs B, Fischer M, Wollmer A, Jostock T, et al. The membrane proximal cytokine receptor domain of the human interleukin-6 receptor is sufficient for ligand binding but not for gp130 association. Journal of Biological Chemistry. 1998;273(33):21374–21379.

[16] Hirabayashi Y, Lemmey A. The role of tocilizumab in the treatment of rheumatoid arthritis. INTECH Open Access Publisher; 2012.

[17] Lindmark E, Diderholm E, Wallentin L, Siegbahn A. Relationship between interleukin 6 and mortality in patients with unstable coronary artery disease: effects of an early invasive or noninvasive strategy. Jama. 2001;286(17):2107–2113.

[18] Bran G, Goette K, Riedel K, Hoermann K, Riedel F. IL-6 antisense-mediated growth inhibition in a head and neck squamous cell carcinoma cell line. In Vivo. 2011;25(4):579–584.

[19] Nilsson MB, Langley RR, Fidler IJ. Interleukin-6, secreted by human ovarian carcinoma cells, is a potent proangiogenic cytokine. Cancer Research. 2005;65(23):10794–10800.

[20] PRIES R, THIEL A, BROCKS C, WOLLENBERG B. Secretion of tumor-promoting and immune suppressive cytokines by cell lines of head and neck squamous cell carcinoma. in vivo. 2006;20(1):45–48.

[21] Boayue K, Gu L, Yeager A, Kreitman R, Findley H. Pediatric acute myelogenous leukemia cells express IL-6 receptors and are sensitive to a recombinant IL6-Pseudomonas exotoxin. Leukemia. 1998;12(2):182–191.

[22] Shkeir O, Athanassiou-Papaefthymiou M, Lapadatescu M, Papagerakis P, Czerwinski MJ, Bradford CR, et al. In vitro cytokine release profile: Predictive value for metastatic potential in head and neck squamous cell carcinomas. Head & neck. 2013;35(11):1542–1550.

[23] Snyers L, De Wit L. Glucocorticoid up-regulation of high-affinity interleukin 6 receptors on human epithelial cells. Proceedings of the National Academy of Sciences. 1990;87(7):2838–2842.

[24] Takizawa H, Ohtoshi T, Ohta K, Yamashita N, Hirohata S, Hirai K, et al. Growth inhibition of human lung cancer cell lines by interleukin 6 in vitro: a possible role in tumor growth via an autocrine mechanism. Cancer research. 1993;53(18):4175–4181.

[25] Mac Gabhann F, Yang MT, Popel AS. Monte Carlo simulations of VEGF binding to cell surface receptors in vitro. Biochimica et Biophysica Acta (BBA)-Molecular Cell Research. 2005;1746(2):95–107.

[26] von Tiedemann B, Bilitewski U. Characterization of the vascular endothelial growth factor–receptor interaction and determination of the recombinant protein by an optical receptor sensor. Biosensors and Bioelectronics. 2002;17(11):983–991.

[27] Mac Gabhann F, Popel AS. Interactions of VEGF isoforms with VEGFR-1, VEGFR-2, and neuropilin in vivo: a computational model of human skeletal muscle. American Journal of Physiology-Heart and Circulatory Physiology. 2007;292(1):H459–H474.

[28] Wang D, Lehman RE, Donner DB, Matli MR, Warren RS, Welton ML. Expression and endocytosis of VEGF and its receptors in human colonic vascular endothelial cells. American Journal of Physiology-Gastrointestinal and Liver Physiology. 2002;282(6):G1088–G1096.

[29] Yen P, Finley SD, Engel-Stefanini MO, Popel AS. A two-compartment model of VEGF distribution in the mouse. PloS one. 2011;6(11):e27514.

[30] Yang E, van Nimwegen E, Zavolan M, Rajewsky N, Schroeder M, Magnasco M, et al. Decay rates of human mRNAs: correlation with functional characteristics and sequence attributes. Genome research. 2003;13(8):1863–1872.